

## Warming of water temperature in spring and nutrient release from sediment in a shallow eutrophic lake

Ryuichiro Shinohara <sup>\*</sup>, Kenji Tsuchiya and Ayato Kohzu

National Institute for Environmental Studies, 16-2 Onogawa, Tsukuba, Ibaraki 305-8506, Japan

<sup>\*</sup>Corresponding author. E-mail: r-shino@nies.go.jp

 RS, 0000-0003-2716-3312

### ABSTRACT

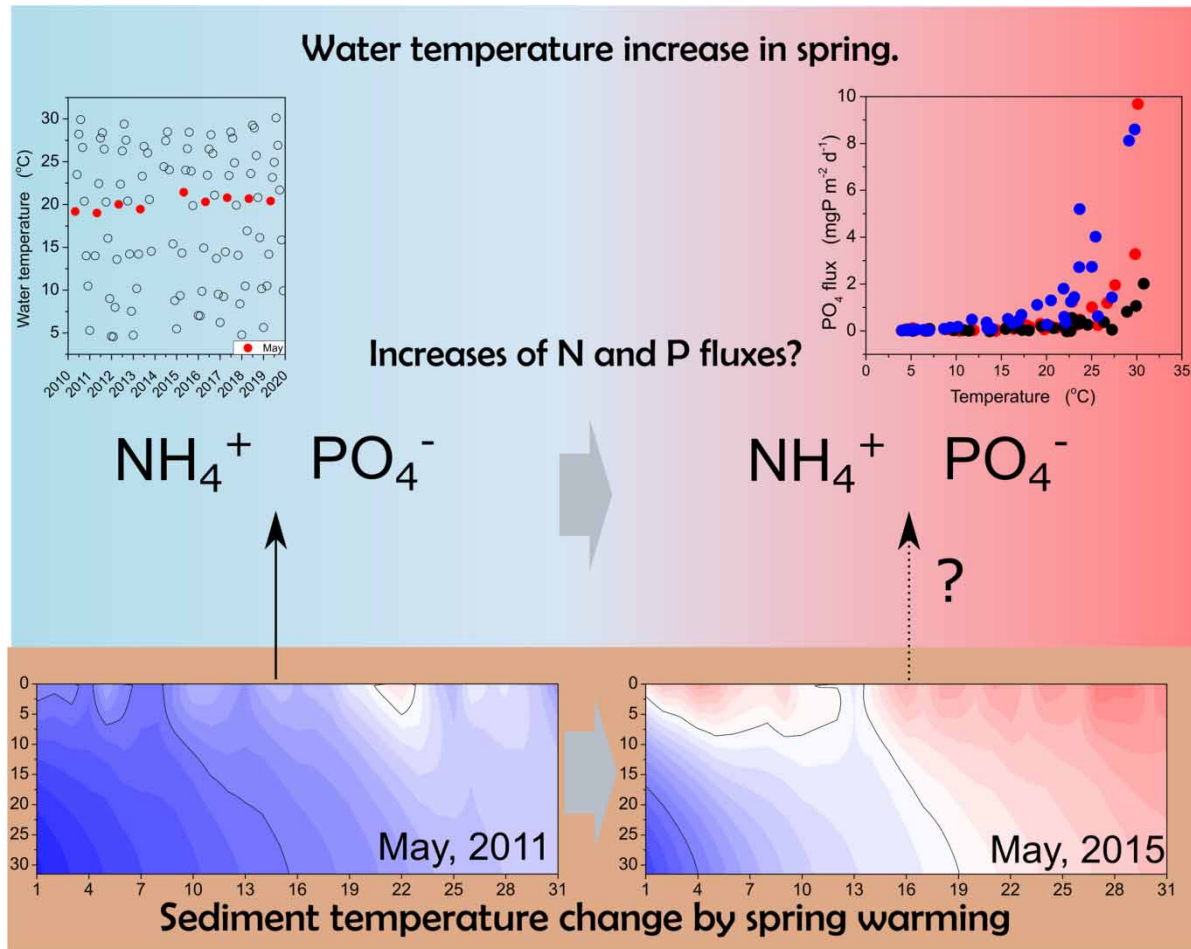
We investigated whether recent springtime water temperature increases in a shallow eutrophic lake affected bottom sediment temperature and fluxes of ammonia ( $\text{NH}_4^+$ ) and phosphate ( $\text{PO}_4^{3-}$ ) from the sediment. We conducted a lake-wide survey of Lake Kasumigaura, Japan, and analyzed the relationship between water temperature increases in spring and  $\text{NH}_4^+$  and  $\text{PO}_4^{3-}$  release fluxes. We also developed a numerical model to analyze how water temperature increase affects sediment temperature. Water temperature in May increased during 2010–2019 at a rate of 1.8–3.2 °C decade<sup>-1</sup>. The numerical simulation results showed that the water temperature increase was accompanied by a sediment temperature increase from a minimum of 18.3 °C in 2011 to a maximum of 21.6 °C in 2015. Despite the substantial difference in the observed sediment temperature (2.9 °C), no significant differences in  $\text{NH}_4^+$  and  $\text{PO}_4^{3-}$  fluxes in May between 2013/2014 and 2015 were found. These results suggest that both water and sediment temperatures are increasing in Lake Kasumigaura in spring, but it is unclear whether this warming has affected  $\text{NH}_4^+$  and  $\text{PO}_4^{3-}$  releases from the sediment. However, because a nonlinear response to sediment temperature was observed, future springtime warming may accelerate  $\text{NH}_4^+$  and  $\text{PO}_4^{3-}$  releases.

**Key words:** nutrient release, sediment temperature, simulation, spring warming

### HIGHLIGHTS

- A water temperature increase was observed in spring by a trend analysis.
- Sediment temperature also increased with the increase of water temperature.
- Ammonia and phosphate releases from bottom sediment were little changed by warming.

## GRAPHICAL ABSTRACT



## INTRODUCTION

Climate warming increases atmospheric temperature, which could also increase the water temperature in lakes (Woolway *et al.* 2019; Woolway *et al.* 2020; Maberly *et al.* 2020) through changing the heat fluxes on the lake surface (Livingstone 2003). Under the RCP8.5 scenario of the Intergovernmental Panel on Climate Change (IPCC 2014), the atmospheric temperature will increase by 4.8 °C by 2100. In deep, well-stratified lakes, an atmospheric temperature increase leads to an increase in epilimnion temperatures (Niedrist *et al.* 2018), whereas in shallow, polymictic lakes, it could increase the whole water column. Therefore, shallow lake sediments are more likely affected by temperature increases than deep lake sediments. For example, O'Reilly *et al.* (2015) have reported that lake surface temperatures around the world have been increasing during 1985 and 2009 (O'Reilly *et al.* 2015).

Sediment temperature is one of the most important parameters for nutrient cycling in lacustrine environments. An increase in sediment temperature, thereby increasing microbial decomposition of organic matter, can accelerate the release of ammonia (NH<sub>4</sub><sup>+</sup>) and phosphate (PO<sub>4</sub><sup>3-</sup>) from the sediment (Rydin *et al.* 2017). Such internal nutrient loading of NH<sub>4</sub><sup>+</sup> and PO<sub>4</sub><sup>3-</sup> promotes phytoplankton blooms in the lake (Yang *et al.* 2020). Release rates of phosphorus (P) from lake sediments are usually highest in summer (Wang *et al.* 2019), but increases in lake water temperatures have been also observed seasonality (Winslow *et al.* 2017). For example, Li *et al.* (2019) observed long-term water temperature in shallow lakes in China during 1979 and 2017. They found that increases in water temperatures are largest during spring and the water temperature increase is associated with an increase in solar radiation (Li *et al.* 2018). A water temperature increase in spring might be expected to enhance effluxes of NH<sub>4</sub><sup>+</sup> and PO<sub>4</sub><sup>3-</sup> from sediment to the overlying water, as given the effects of temperatures on PO<sub>4</sub><sup>3-</sup> release

(Holdren & Armstrong 1980; Jensen & Andersen 1992). However, despite many studies of water temperature increases due to global warming (Chikita *et al.* 2018; Chikita *et al.* 2019), little information is available about how spring warming is changing sediment temperature and consequent releases of  $\text{NH}_4^+$  and  $\text{PO}_4^{3-}$  from sediment.

This study addressed the following questions about the effects of a water temperature increase on bottom sediments of shallow lakes: (1) Have increased water temperatures been changing sediment temperatures, thereby making the release of nutrients from lake sediments into the overlying water more likely? and (2) How do N and P releases from bottom sediments respond to water temperature increases? If springtime warming increases the  $\text{NH}_4^+$  and  $\text{PO}_4^{3-}$  release rates, the duration of the  $\text{NH}_4^+$  and  $\text{PO}_4^{3-}$  releases period could be extended and accelerate eutrophication.

We hypothesized that (1) the long-term water temperature increase in spring has increased the sediment temperature; and (2) the sediment temperature increase is enhancing nitrogen (N) and P fluxes from sediments. To test these hypotheses, we studied springtime water and sediment temperature trends and  $\text{NH}_4^+$  and  $\text{PO}_4^{3-}$  fluxes from the bottom sediment in Lake Kasumigaura, Japan. Lake Kasumigaura is a shallow, hypereutrophic lake, and P released from the bottom sediment accounts for approximately half of the total P loading. In the lake, empirically, water temperature is highest in summer, more than 30 °C every year, and  $\text{NH}_4^+$  and  $\text{PO}_4^{3-}$  also exhibit maximum releases during summer. First, we analyzed water temperature changes in the lake from 2010 to 2019 to clarify whether and how much water temperature increased during this period. Next, we developed a one-dimensional numerical model to analyze how sediment temperature has been changing in Lake Kasumigaura from 2010 to 2019 in response to the water temperature increase. We simulated sediment temperatures and compared them between the years in which the minimum and maximum water temperatures were recorded in the lake. Finally, we analyzed the relationship between observed sediment temperatures and  $\text{NH}_4^+$  and  $\text{PO}_4^{3-}$  fluxes from the sediment to the water during three consecutive years (2013–2015) and examined whether the increase in sediment temperature also increased  $\text{NH}_4^+$  and  $\text{PO}_4^{3-}$  releases. The loadings from the inflow rivers as well as the factors changing the  $\text{NH}_4^+$  and  $\text{PO}_4^{3-}$  releases in August were also discussed.

## METHODS

### Lake Kasumigaura

Lake Kasumigaura is the second largest lake in Japan, with an area of 171 km<sup>2</sup>, a mean depth of approximately 4 m, and a maximum depth of 7.4 m (Figure 1). This lake is a polymictic lake, showing vertical mixing every day in the water column. The average water residence time is approximately 200 days. More than 900,000 people live in the lake's watershed (1,577 km<sup>2</sup>), and the lake is the source of drinking water for about 660,000 people. Land use in the watershed is 30%

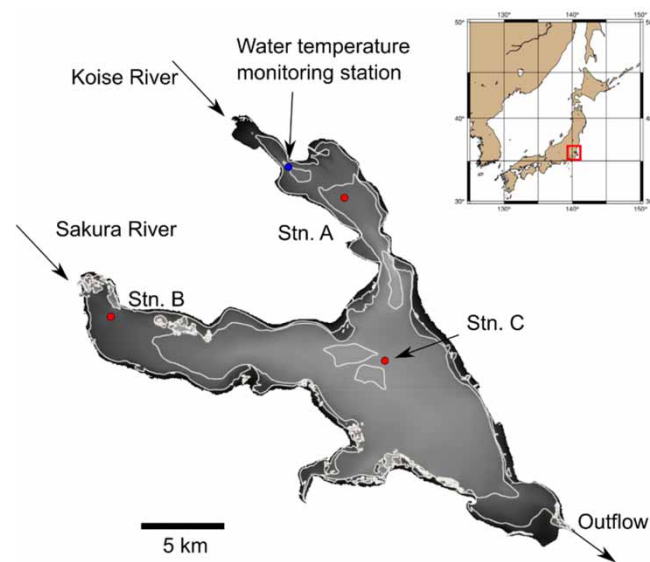


**Figure 1** | Map of Lake Kasumigaura and locations of sediment sampling stations, Stn. A, B, and C. Water temperatures At Stn. B and Stn. C, water temperatures were monitored at positions very close to the sediment sampling sites.

forest, 25% paddy field, 25% ploughed field, 10% residential, and 10% other. Extremely high loads of organic matter and nutrients have caused eutrophication of the lake, which has mean concentrations of total nitrogen (TN) and total phosphorus (TP) of  $0.78 \text{ mgN L}^{-1}$  and  $0.08 \text{ mgP L}^{-1}$ , respectively, as measured at the center of the lake in 2018.

### Sediment and water sampling and sediment temperature measurements

Sediment samples were collected monthly from December 2012 to December 2015 at three sampling stations (Stns. A, B, and C; Figure 1), each in a different area of the lake (Matsuoka *et al.* 1986). The sediment samples were collected under calm conditions with low wind speed. At Stn. A, water depth 4.0 m, is in organic-rich sediments derived from the inflow of the Koise River. At Stn. B, water depth 2.0 m, the sediments include coarser particles derived from dredging (Tsuchiya *et al.* 2020). At Stn. C, in the center of the lake, the water depth is 6.0 m; thus, it was the deepest sampling site. The detailed physical properties of the sediments at each station are described in the supporting information (Supplementary Material, Table S1).

A gravity core sampler ( $\phi = 11 \text{ cm}$ ) was used for collecting sediment samples. Just after each sediment core was collected, we used a syringe to collect a water sample just above the bottom sediment for later analysis of  $\text{NH}_4^+$  and  $\text{PO}_4^{3-}$ . In addition, at each station, we measured the sediment temperature at 1.5, 4.5, 7.5, 10.5, 13.5, 16.5, 19.5, 22.5, 25.5, 28.5, and 31.5 cm depth below the sediment surface with a digital thermometer (TX10-01, Yokogawa, Tokyo, Japan). A duplicate core was taken to the laboratory as soon as possible for analysis of  $\text{NH}_4^+$  and  $\text{PO}_4^{3-}$  concentrations in the surface sediment.

We measured dissolved oxygen (DO), and pH *in situ* at a point just above the lake bottom with a multiparameter water quality sonde (Hydrolab DS5, HydroMet, Loveland, Colorado, USA). We also collected water samples for analysis of chlorophyll *a* (Chl-*a*) in a well-washed, 2-m column sampler (Rigo Co., Tokyo, Japan). The collected water samples were transported to our laboratory within  $\sim 2 \text{ h}$ .

The water samples of the two major inflow rivers (the Sakura and Koise Rivers) were also collected monthly from January 2014 to December 2015. The sampling point of the Sakura River was approximately 10 km upstream from Lake Kasumigaura. The sampling point of the Koise River was 9.5 km upstream from Lake Kasumigaura. We collected surface water by using a well-washed container (5 L) from the bridge. The collected water was stored in an acid-washed polycarbonate container (2 L) and carried to our laboratory as soon as possible ( $\sim 2 \text{ h}$ ).

In the laboratory, each sediment core (0–1.5 cm depth) was sliced at a depth of 0.75 cm under an  $\text{N}_2$  atmosphere for analysis of  $\text{NH}_4^+$  and  $\text{PO}_4^{3-}$  in the porewater. We centrifuged (relative centrifugal force, 2,278 *g*) each sample for 15 min at  $4 \text{ }^\circ\text{C}$  and filtered the supernatant through a GF/F glass fiber filter (nominal pore size:  $0.70 \text{ }\mu\text{m}$ ) under an  $\text{N}_2$  atmosphere. The filtrates were then frozen ( $-20 \text{ }^\circ\text{C}$ ) and stored until analysis. Each water sample (200 mL) for Chl-*a* analysis was immediately filtered through a GF/F glass fiber filter, and then the filter was frozen and stored at  $-20 \text{ }^\circ\text{C}$  until analysis.

### Water temperature and river flow rate data

Hourly water temperature data were downloaded from the Water Information System of the Ministry of Land, Transportation, and Tourism (<http://www1.river.go.jp/>). Our sediment sampling point at Stn. A was a distance of 2.4 km from the water temperature observation site (Figure 1), but we expected the difference in water temperature between the two sites to be small, based on our observations. We used water temperature data from 2010 to 2019 for analyzing the change in monthly averaged water temperature. The flow rates ( $\text{m}^3 \text{ s}^{-1}$ ) from the Sakura and Koise Rivers were provided by the Ministry of Land, Transportation, and Tourism.

### Chemical analysis

$\text{NH}_4^+$  and  $\text{PO}_4^{3-}$  concentrations were analyzed with an auto-analyzer (QuAatro 2-HR, BLTec, Tokyo, Japan) according to the manufacturer's instructions. Briefly, the  $\text{NH}_4^+$  concentration was analyzed by a phenate method (4,500- $\text{NH}_3 \text{ F}$ ; APHA 2005), and the  $\text{PO}_4^{3-}$  concentration was analyzed by a molybdenum blue method (Murphy & Riley 1962). The minimum detection limits ( $3\sigma$  of the 6 blanks) of  $\text{NH}_4^+$  and  $\text{PO}_4^{3-}$  were  $1.0 \text{ }\mu\text{gN L}^{-1}$  and  $0.8 \text{ }\mu\text{gP L}^{-1}$ , respectively. Chl-*a* was extracted by methanol, and the optical densities were determined by spectrophotometer (UV-2500PC, Shimadzu, Kyoto, Japan). The data were opened online at the Kasumigaura Database of the National Institute for Environmental Studies.

### N and P release from sediment to the overlying water

In the present study, molecular diffusion from the sediment to the water was assumed to occur with little physical disturbance. Although Lake Kasumigaura is a shallow lake, the collection of sediment samples was not under any strong physical disturbance (Matsuzaki *et al.* 2021). We calculated the  $\text{NH}_4^+$  and  $\text{PO}_4^{3-}$  release flux *J* from the N and P data of

the bottom water (+0 cm) and the porewater (0.75 cm depth) using the following equation (Klump & Martens 1981):

$$J = -\phi D \frac{\partial C}{\partial z} \quad (1)$$

where  $\phi$  is porosity (dimensionless),  $D$  is the tortuosity-corrected diffusion coefficient ( $\text{cm}^2 \text{s}^{-1}$ ),  $C$  is the  $\text{NH}_4^+$  or  $\text{PO}_4^{3-}$  concentration ( $\mu\text{g cm}^3$ ), and  $z$  is sediment depth.  $D$  was calculated as follows (Reddy & DeLaune 2008):

$$D = \frac{1}{1 - \ln(\phi^2)} D_m \quad (2)$$

where  $D_m$  is the molecular diffusion coefficient ( $\text{cm}^2 \text{s}^{-1}$ ). For the  $D_m$  values of  $\text{NH}_4^+$  and  $\text{PO}_4^{3-}$  in Equation (2), we used the values for 18 °C of  $1.68 \times 10^{-5}$  and  $7.15 \times 10^{-6} \text{ cm}^2 \text{ s}^{-1}$ , respectively, determined by Li & Gregory (1974). We then used the Stokes-Einstein relationship to calculate the diffusion coefficients at temperatures other than 18 °C:

$$\frac{\mu_1 D_1}{T_1} = \frac{\mu_2 D_2}{T_2} \quad (3)$$

where  $\mu_1$  and  $\mu_2$  are viscosities, and  $D_1$  and  $D_2$  are molecular diffusion coefficients at temperatures  $T_1$  and  $T_2$  (K), respectively.

### Numerical modeling of sediment temperature

The sediment temperature simulation model was based on one-dimensional diffusion following (Pivato *et al.* 2018):

$$\frac{\partial T}{\partial t} = \frac{\lambda}{\rho c} \frac{\partial^2 T}{\partial z^2} \quad (4)$$

where  $T$  is sediment temperature (°C),  $t$  is time (s),  $\lambda$  is thermal conductivity ( $\text{W cm}^{-1} \text{K}^{-1}$ ),  $\rho$  is the density of the water or sediments ( $\text{g cm}^{-3}$ ), and  $c$  is the specific heat of sediment ( $\text{J g}^{-1} \text{K}^{-1}$ ). The values of  $\rho$  (for the sediments) and  $\lambda$  are given in the supporting information (Supplementary Material, Table S1). Thermal conductivity was set at  $0.25 \times 10^{-2} \text{ W cm}^{-1} \text{K}^{-1}$  or  $0.30 \times 10^{-2} \text{ W cm}^{-1} \text{K}^{-1}$  (Hipsey *et al.* 2019), based on the organic-rich sediments of Lake Kasumigaura. An implicit finite difference scheme was used to solve Equation (4). The calculations were conducted for the sediment layer from 0 to 31.5 cm depth at depth intervals ( $\Delta z$ ) of 0.25 cm. For the boundary condition at the top of the sediment, we used the monthly water temperature data collected at each station. We compared the hourly data with observed water temperature data (Supplementary Material, Figure S1), and the regression equation was applied to the boundary conditions. The time interval ( $\Delta t$ ) of the calculation was 1,800 s.

To validate the model, we used the temperatures measured in December 2012 and December 2013 and calculated the root mean square error (RMSE) between the calculated and observed values as follows:

$$RMSE = \sqrt{\frac{1}{n} \sum_{i=1}^n (x_{cal} - x_{obs})^2} \quad (5)$$

where  $n$  is the number of data,  $x_{cal}$  is the calculated temperature, and  $x_{obs}$  is the observed sediment temperature (°C).

To calculate the heat flux between sediment and water, we used the following equation (Fang & Stefan 1996):

$$H_G = \lambda \frac{T_w - T_s}{\Delta z} \quad (6)$$

where  $H_G$  is the heat flux ( $\text{W m}^{-2}$ ) between sediment and the water column,  $T_w$  and  $T_s$  are water and sediment temperatures (°C), respectively, and  $\Delta z$  is the depth interval in the model (0.25 cm).

## Numerical calculation of cool and warm years

We calculated the differences in sediment temperature and heat flux between 2011, when water temperatures were relatively cool, and 2015, when they were warm (see section Long-term water temperatures). The initial conditions were set as constant values of water temperature, and the model spin-up period was 2 months. Missing data were linearly interpolated using the data collected before and after.

## Statistical analysis

For long-term trend analyses and validation of the numerical simulations, we used the Pearson product moment correlation coefficient. We used paired *t*-tests to assess differences in sediment temperature and the release fluxes of  $\text{NH}_4^+$  and  $\text{PO}_4^{3-}$ . A type I error ( $\alpha$ ) of less than 0.05 was regarded as significant. We used Microcal Origin ver. 8.5.1.J software for the statistical analyses.

## RESULTS

### Long-term water temperatures

Monthly mean water temperatures at the three stations are shown in Figure 2. Note that water temperatures recorded in February are not shown, because many data were missing. Spring water temperatures (March–May) increased at rates of 1.8–3.2 °C decade<sup>-1</sup> from 2010 to 2019 (Figure 2 and Supplementary Material, Figure S2). In particular, the water temperature in May increased at all three stations. The monthly mean water temperature in May was lowest in 2011 (Stn. A: 19.6 °C, Stn. B: 18.9 °C, and Stn. C: 19.0 °C) and highest in 2015 (Stn. A: 22.9 °C, Stn. B: 22.1 °C, and Stn. C: 21.4 °C). Therefore, these years were used to represent cool and warm years, respectively, in this study.

### Numerical model validation and analysis

The developed one-dimensional numerical model successfully simulated the sediment temperature of Lake Kasumigaura during 2012–2013 (Supplementary Material, Figure S3). The measured and calculated sediment temperatures differed only slightly (Stn. A, RMSE = 0.98 °C; Stn. B, RMSE = 1.1 °C; Stn. C, RMSE = 1.1 °C), and the correlation coefficient for the relation between the observed and simulated values was high at all stations (Supplementary Material, Figure S4; Stns. A–C:  $r = 0.99$ ,  $p < 0.001$ ).

Differences in sediment temperatures between 2011 and 2015 were simulated by the numerical model (Figure 3), and particularly for those in May of both years (Figure 4). The monthly mean water temperature difference in May between 2011 and 2015 was 3.3 °C at Stn. A, 3.2 °C at Stn. B, and 2.4 °C at Stn. C. The calculated sediment temperature at 0.75 cm depth in May increased from 18.3 to 21.4 °C at Stn. A, 18.6 to 21.6 °C at Stn. B and 18.9 to 20.1 °C at Stn. C between 2011 and 2015 (Figure 4). The 25-h running mean of the heat flux between sediment and water ranged between –12 and 14 W m<sup>-2</sup> in both 2011 and 2015 (Figure 3(j)–3(l)).

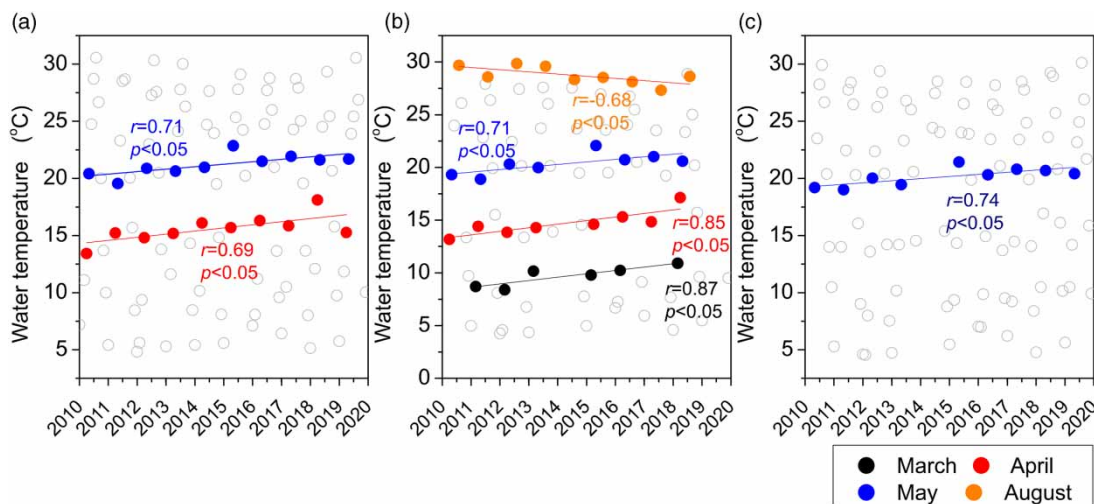


**Figure 2** | Monthly mean water temperature fluctuations in Lake Kasumigaura at (a) Stn. A, (b) Stn. B, and (c) Stn. C. The colored circles are values for months showing statistically significant relationships between water temperature and year. The correlation coefficient (*r*) and the *p*-values are also shown.

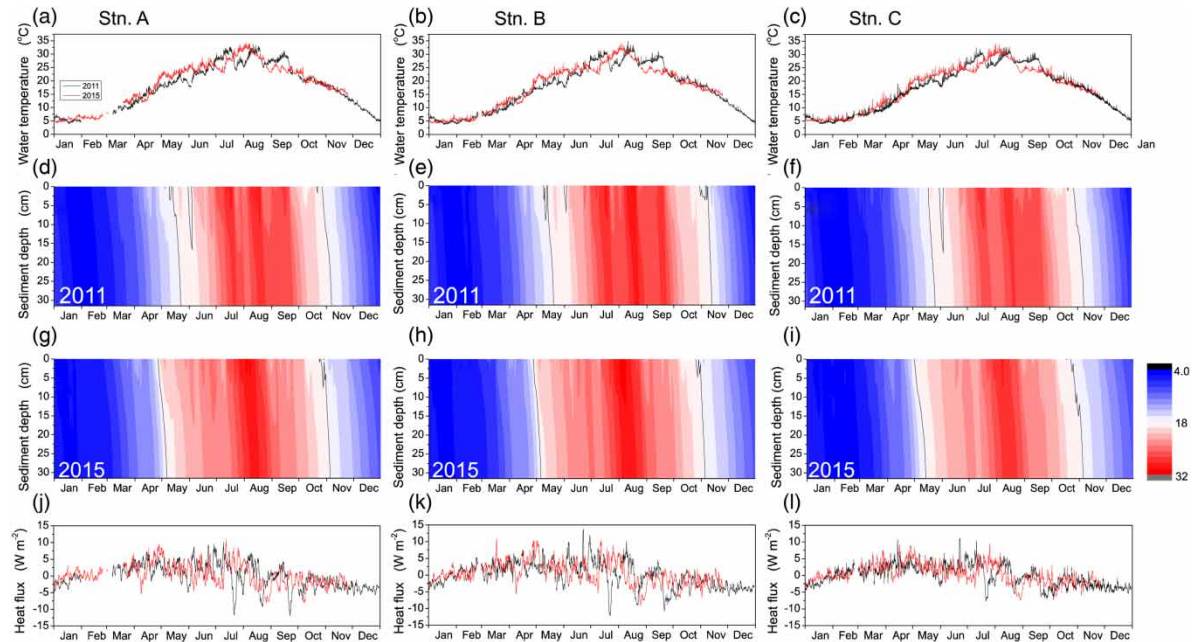


**Figure 3** | (a–c) Water temperature fluctuations in 2011 (black lines) and 2015 (red lines), simulation results for sediment temperatures (color scale, °C) in (d–f) 2011 and (g–i) 2015, and (j–l) heat fluxes (25 h running mean) in 2011 (black lines) and 2015 (red lines) at stations A–C. The positive values mean the downward flux. Please refer to the online version of this paper to see this figure in colour: <http://dx.doi/10.2166/wcc.2021.145>.

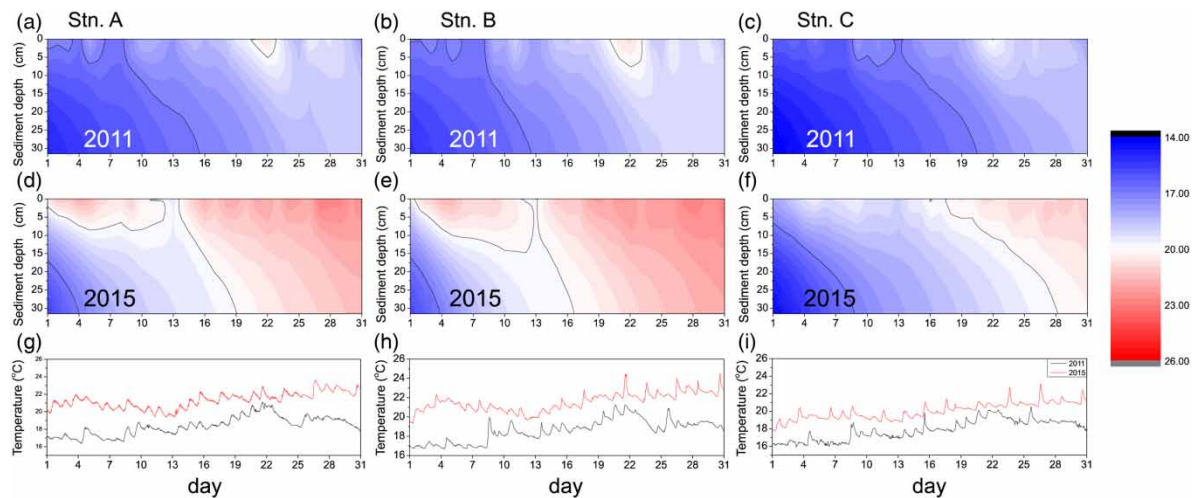


**Figure 4** | Time series of sediment temperature (color scale, °C) in May of (a–c) 2011 and (d–f) 2015 at station A–C. (g–i) Time series of sediment temperature at 0.75 cm depth at Stn. A–C. Please refer to the online version of this paper to see this figure in colour: <http://dx.doi/10.2166/wcc.2021.145>.

### Changes in temperature and N and P releases from sediment during 2013–2015

The release rates of  $\text{NH}_4^+$  and  $\text{PO}_4^{3-}$  ranged from 0.59 to 95  $\text{mgN m}^{-2} \text{d}^{-1}$  for  $\text{NH}_4^+$  and from  $-0.02$  to 11  $\text{mgP m}^{-2} \text{d}^{-1}$  for  $\text{PO}_4^{3-}$  (Figure 5). The fluxes increased with increasing sediment temperature, and the correlation coefficients between fluxes and sediment temperature were high (Supplementary Material, Table S2). The response of the release rates to sediment temperature differed among the stations, and remarkably the response of the  $\text{NH}_4^+$  flux was linear except at Stn. A. By contrast, at all stations, the  $\text{PO}_4^{3-}$  flux from the sediment did not begin to increase until the sediment temperature exceeded 15–20 °C (Figure 5).

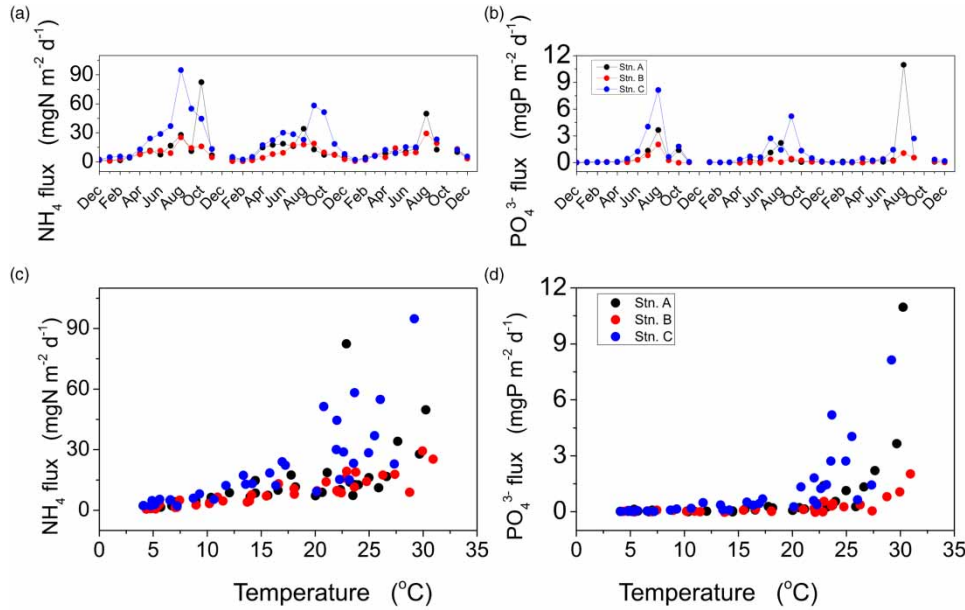


**Figure 5** | Time series of (a)  $\text{NH}_4^+$  and (b)  $\text{PO}_4^{3-}$  fluxes from December 2012 to December 2015. Relationships between (c)  $\text{NH}_4^+$  and (d)  $\text{PO}_4^{3-}$  fluxes from sediment and sediment temperature in Lake Kasumigaura at stations A–C.

Comparison of the  $\text{NH}_4^+$  and  $\text{PO}_4^{3-}$  fluxes in May between 2013/2014 and 2015 by paired *t*-tests showed no significant difference in either the  $\text{NH}_4^+$  or the  $\text{PO}_4^{3-}$  flux between 2013/2014 and 2015, even though the sediment temperature was significantly higher, by 2.9 °C, in 2015 compared with 2013/2014 (Table 1).

Sediment temperature better explained the  $\text{NH}_4^+$  and  $\text{PO}_4^{3-}$  fluxes from the sediment to the overlying water than the other measured parameters, including phytoplankton biomass (Chl-*a* concentration) and the DO concentration and pH at the lake bottom, as indicated by the high correlation coefficients between sediment temperature and both fluxes (Table 2). Chl-*a*, DO, and pH all varied greatly during 2012–2015 (Figure 6), but DO concentrations were high ( $>7.2 \text{ mg L}^{-1}$ ) in May at all stations.

**Table 1** | Results of paired *t*-tests comparing sediment temperature with  $\text{NH}_4^+$  and  $\text{PO}_4^{3-}$  fluxes between May 2013/2014 and May 2015

Year	Temperature (°C)		$\text{NH}_4^+$ flux ( $\text{mgN m}^{-2} \text{d}^{-1}$ )		$\text{PO}_4^{3-}$ flux ( $\text{mgP m}^{-2} \text{d}^{-1}$ )	
	2013	2015	2013	2015	2013	2015
Average	17.7	20.6	15.5	10.8	0.23	0.2
<i>t</i> -test	$t = 4.3, p < 0.001$		$t = 4.3, p = 0.47$		$t = 4.3, p = 0.77$	
Year	2014	2015	2014	2015	2014	2015
Average	17.7	20.6	15.9	10.8	0.33	0.2
<i>t</i> -test	$t = 4.3, p < 0.001$		$t = 4.3, p = 0.47$		$t = 4.3, p = 0.50$	

The averaged values of Stns. A, B, and C are shown.

**Table 2** | Correlation coefficients for the relationship between  $\text{PO}_4^{3-}$  and  $\text{NH}_4^+$  fluxes and chlorophyll *a* (Chl-*a*), dissolved oxygen (DO), or pH and sediment temperature (\*\* $p < 0.001$ )

	Chl- <i>a</i>	DO	pH	Temperature
$\text{PO}_4^{3-}$ flux	0.29**	-0.68**	-0.01	0.79**
$\text{NH}_4^+$ flux	0.18	-0.51**	-0.09	0.63**

Note that the natural logarithm of the  $\text{PO}_4^{3-}$  flux was compared with sediment temperature (see Supplementary Material, Table S2).



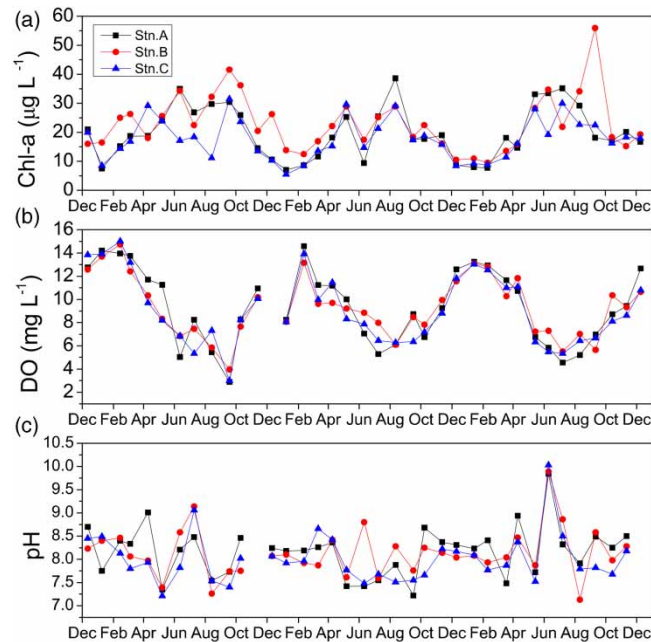


**Figure 6** | Time series of (a) chlorophyll a (Chl-a), (b) dissolved oxygen (DO), and (c) pH in the bottom water at Stns. A–C from December 2012 to December 2015.

### $\text{PO}_4^{3-}$ and $\text{NH}_4^+$ fluxes from the inflow rivers

The flow rates of the Sakura and Koise Rivers and the  $\text{NH}_4^+/\text{PO}_4^{3-}$  concentrations during 2014 and 2015 are shown in Figure 7. The  $\text{NH}_4^+$  concentrations were, on average,  $0.06 \text{ mgN L}^{-1}$ , and the averaged  $\text{PO}_4^{3-}$  concentration was  $0.009 \text{ mgP L}^{-1}$  in the Sakura River. In the Koise River, the concentrations were higher than the Sakura River. The averaged  $\text{NH}_4^+$  concentration was  $0.24 \text{ mgN L}^{-1}$ , whereas the averaged  $\text{PO}_4^{3-}$  concentration was  $0.019 \text{ mgP L}^{-1}$ .

We calculated the fluxes of  $\text{NH}_4^+$  and  $\text{PO}_4^{3-}$  from the inflow rivers by using these values in May. Because the basin area of Stn. A was  $23 \text{ km}^2$  (Matsuoka *et al.* 1986), the estimated  $\text{NH}_4^+$  and  $\text{PO}_4^{3-}$  fluxes from the Koise River in May 2014 were  $1.73 \text{ mgN m}^{-2} \text{ d}^{-1}$  and  $0.23 \text{ mgP m}^{-2} \text{ d}^{-1}$ , respectively. By contrast, the fluxes from the Sakura River (the area:  $49.3 \text{ km}^2$ ) in May 2014 were  $0.60 \text{ mgN m}^{-2} \text{ d}^{-1}$  for  $\text{NH}_4^+$  and  $0.15 \text{ mgP m}^{-2} \text{ d}^{-1}$ . From the Koise River, the fluxes in 2015 were  $1.63 \text{ mgN m}^{-2} \text{ d}^{-1}$  for  $\text{NH}_4^+$  and  $0.24 \text{ mgP m}^{-2} \text{ d}^{-1}$  for  $\text{PO}_4^{3-}$ . The fluxes from the Sakura River were  $1.39 \text{ mgN m}^{-2} \text{ d}^{-1}$  for  $\text{NH}_4^+$  and  $0.17 \text{ mgP m}^{-2} \text{ d}^{-1}$  for  $\text{PO}_4^{3-}$ . The  $\text{NH}_4^+$  flux from the sediment at Stn. A were 8.4 times greater than from the Koise River, whereas the  $\text{NH}_4^+$  flux from the Sakura River was 7.8 times greater than from the sediment at Stn. B during 2014 and 2015. The  $\text{PO}_4^{3-}$  flux from the sediment at Stn. A was 3.2 times greater than from the Koise River, whereas it was 1.6 times greater Stn. B than from the Sakura River. However, in 2015, discharges of total N and total P into the lake from rivers (e.g.,  $34.9 \text{ mgN m}^{-2} \text{ d}^{-1}$  and  $1.37 \text{ mgP m}^{-2} \text{ d}^{-1}$  from the Koise River at Stn. A) were much greater than the fluxes of  $\text{NH}_4^+$  ( $10.8 \text{ mgN m}^{-2} \text{ d}^{-1}$ ) and  $\text{PO}_4^{3-}$  ( $0.20 \text{ mgP m}^{-2} \text{ d}^{-1}$ ) from the bottom sediment in May.

## DISCUSSION

The most striking finding of this study is that in Lake Kasumigaura, although springtime water temperatures increased, the increase had no effect or only a limited effect on N and P effluxes from the sediment. The water temperature increase in spring is consistent with observations at other shallow lakes in temperate regions (Li *et al.* 2019), but to our knowledge this is the first study to assess the effects of lake water warming on sediment N and P in the spring season. Summertime warming is often considered (O'Reilly *et al.* 2015), but our study observed springtime warming of water temperature and the effects on the sediment.

Our simulation results also indicated warming of sediment temperature in spring, but the increase was too small to affect N and P release fluxes from the sediment to the overlying water, as shown by the lack of significant changes in  $\text{NH}_4^+$  and  $\text{PO}_4^{3-}$

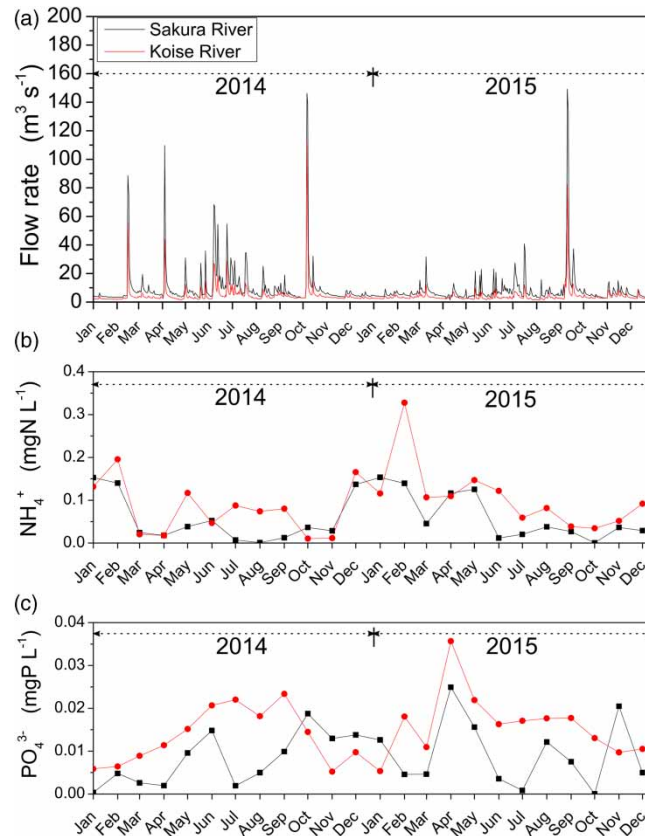


**Figure 7** | The daily flow rates from the inflow river (the Sakura and Koise Rivers) and  $\text{NH}_4^+$  and  $\text{PO}_4^{3-}$  concentrations in the inflow river from 2014 to 2015.

fluxes in May between 2013 or 2014 and May 2015 (Figure 5; Table 1). The  $\text{NH}_4^+$  and  $\text{PO}_4^{3-}$  releases from sediment were much smaller than the fluxes of total N and total P from the inflow river.

The limited effect of warmer springtime temperatures on the releases of N and P from sediment has several possible explanations. First, acceleration of microbial decomposition of organic P may have been insufficient. Decomposition of organic P, especially DNA-P, is mainly responsible for the release of P from sediment to the overlying water (Reitzel *et al.* 2007; Ishii *et al.* 2010). Second, oxidation and reduction potentials affect the acceleration. P in sediment, which is often adsorbed onto metal oxyhydroxides, is released under reductive conditions (Chen *et al.* 2018). However, the observed DO concentrations in the water column in May ( $7.2 \text{ mg L}^{-1}$ ; Figure 6) indicate oxidative conditions.

The effects of warmer springs on  $\text{NH}_4^+$  and  $\text{PO}_4^{3-}$  fluxes are still unclear, but the nonlinear increase in the  $\text{PO}_4^{3-}$  flux in relation to sediment temperature suggests that a further increase in temperature might accelerate the flux. Gudasz *et al.* (2010) have reported that warming of water temperature in lakes accelerates the decomposition and mineralization of organic matter (Gudasz *et al.* 2010). The  $\text{PO}_4^{3-}$  supply to sediment porewater depends not only on the mineralization of organic P but also on the presence or absence of electron acceptors (Schindler 2012) and sulfate-reducing bacteria (Caraco *et al.* 1989). Sediment temperature should also affect these reactions related to  $\text{PO}_4^{3-}$  and organic P.

Masunaga & Komuro (2019) have reported that heat fluxes at the lake surface cannot fully explain water temperatures in Lake Kasumigaura (Masunaga & Komuro 2019). They suggested that the sediment acts as a heat buffer and that the heat flux between sediment and water can be as large as  $100 \text{ W m}^{-2}$  in summer. However, our numerical simulation results for sediment temperature are inconsistent with this suggestion (Figure 3). A heat flux of  $14 \text{ W m}^{-2}$  resulted in an increase of the water temperature of Lake Kasumigaura of approximately  $0.072 \text{ }^\circ\text{C}$  per day ( $\sim 2.2 \text{ }^\circ\text{C}$  per month). This increase is too small, compared to the heat flux at the water surface, to account for the water temperature changes in Lake Kasumigaura (Sugita *et al.* 2020). The small heat flux between the sediment and the water column was consistent with the other lakes (Fang & Stefan 1996).

Several factors may account for the changing water temperature of Lake Kasumigaura. An increase in solar radiation, possibly associated with global brightening and dimming (Wild *et al.* 2005; Tanaka *et al.* 2016), may explain increases in water temperature globally (Fink *et al.* 2014) and also in Lake Kasumigaura. Sugita *et al.* (2014) have shown that wind direction and speed change the latent heat flux, which can cause water temperature fluctuations (Sugita *et al.* 2014). In this study, a water temperature in May of around 20 °C was the turning point for the release of P from sediment (Figure 5); this result implies that a further increase of water temperature in spring may cause greater releases of  $\text{NH}_4^+$  and  $\text{PO}_4^{3-}$  from the sediment.

We could not determine whether spring warming has been observed in other lakes, but global brightening and dimming have been observed all over the world (Wild 2009; Cermak *et al.* 2010). Global brightening and dimming could be caused by the decrease in aerosol (Wild *et al.* 2005) and such brightening also increases shortwave radiation on the lake surface (Fink *et al.* 2014). The future meteorology, including air temperature and precipitation, is unclear now, but for a more comprehensive understanding of spring warming, the factors responsible for the changing water temperature in other lakes in the world in May must be clarified so that future water temperatures in May can be predicted.

In this study, the mechanisms causing the changes in  $\text{NH}_4^+$  and  $\text{PO}_4^{3-}$  fluxes with the changes in surface water and sediment temperatures were not examined. The relationship between  $\text{PO}_4^{3-}$  releases and sediment temperature, which differed among the stations (Figure 5), may depend on sediment characteristics. For example, the sandy sediment at Stn. B had a lower organic matter content than the sediment at the other stations (Tsuchiya *et al.* 2020; Supplementary Material, Table S1) and release rates of  $\text{NH}_4^+$  and  $\text{PO}_4^{3-}$  there were low, even at high temperatures. Furthermore, the relationship between  $\text{SO}_4^{2-}$  and  $\text{PO}_4^{3-}$  needs further investigation. The clear decrease in  $\text{SO}_4^{2-}$  concentration with the sediment depth suggests that  $\text{SO}_4^{2-}$  reduction and pyrite formation could occur in the sediments (Gächter & Müller 2003) because pyrite was also detected in Lake Kasumigaura (Supplementary Material, Figures S5 and S6). Pyrite does not adsorb  $\text{PO}_4^{3-}$  onto the sediment solids (Gächter & Müller 2003).  $\text{SO}_4^{2-}$  and  $\text{PO}_4^{3-}$  should be addressed in the future work because they could be involved in the P release from the bottom sediments (Sinkko *et al.* 2011).

The higher temperature could also change N cycling in the lake, such as denitrification (Veraart *et al.* 2011). In the case of Lake Kasumigaura, the undetectable level of  $\text{NO}_3^-$  concentrations in the sediment porewater could have resulted from denitrification in the bottom sediments regardless of the seasons (Supplementary Material, Figure S5). Further investigation is warranted about the impacts of temperature increase on N cycles in the watershed.

## CONCLUSION

We analyzed the effect of increases in water temperature in spring on bottom sediment temperature and the potential impact on the release of  $\text{NH}_4^+$  and  $\text{PO}_4^{3-}$  from the sediment to the overlying water. Water temperature in spring has been increasing in Lake Kasumigaura. We used a numerical model to examine changes in sediment temperature due to the warming of the water during 2010–2019 and found that sediment temperature in May was approximately 3.1 °C higher in 2015, a warm year, compared with 2011, a relatively cool year. At Lake Kasumigaura, the  $\text{PO}_4^{3-}$  flux did not start to increase until the sediment temperature reached 15–20 °C. The impact of an increase of sediment temperature in spring is thus still obscure. However, the nonlinear response of the  $\text{PO}_4^{3-}$  flux to sediment temperature suggests that future warming in spring may accelerate the release of  $\text{PO}_4^{3-}$  from sediment. Although the total N flux from the bottom sediment was less than the inflow river, the amount of  $\text{NH}_4^+$  flux from the bottom sediment was, in particular, 8.4 times greater than that from the Koise River. Such a large amount of flux could mitigate the N limitation in particular at Stn. A (Matsuzaki *et al.* 2018). A better understanding of the effects of spring warming will require intensive monitoring of meteorology and water/sediment temperatures during spring.

## ACKNOWLEDGEMENTS

This research was financially supported by KAKENHI (19K04629). We also thank laboratory members Noriko Sugiyama and Yasushi Yakabe for their support in analyzing the ammonia and phosphate concentrations in the sediment porewater. We also thank Shin-ichiro Matsuzaki for the fruitful discussion we exchanged.

## DATA AVAILABILITY STATEMENT

All relevant data are available from an online repository or repositories (<https://db.cger.nies.go.jp/gem/moni-e/inter/GEMS/database/kasumi/index.html>).

## REFERENCES

- APHA 2005 *Standard Methods for the Examination of Water and Wastewater*. American Public Health Association (APHA), Washington, DC, USA.
- Caraco, N., Cole, J. & Likens, G. 1989 Evidence for sulphate-controlled phosphorus release from sediments of aquatic systems. *Nature* **341** (6240), 316–318.
- Cermak, J., Wild, M., Knutti, R., Mishchenko, M. I. & Heidinger, A. K. 2010 Consistency of global satellite-derived aerosol and cloud data sets with recent brightening observations. *Geophysical Research Letters* **37** (21), L21704.
- Chen, M., Ding, S., Chen, X., Sun, Q., Fan, X., Lin, J., Ren, M., Yang, L. & Zhang, C. 2018 Mechanisms driving phosphorus release during algal blooms based on hourly changes in iron and phosphorus concentrations in sediments. *Water Research* **133**, 153–164.
- Chikita, K. A., Oyagi, H., Aiyama, T., Okada, M., Sakamoto, H. & Itaya, T. 2018 Thermal regime of a deep temperate lake and its response to climate change: Lake Kuttara, Japan. *Hydrology* **5** (1), 17.
- Chikita, K., Ochiai, Y., Oyagi, H. & Sakata, Y. 2019 Geothermal linkage between a hydrothermal pond and a deep lake: Kuttara Volcano, Japan. *Hydrology* **6** (1), 4.
- Fang, X. & Stefan, H. G. 1996 Dynamics of heat exchange between sediment and water in a lake. *Water Resources Research* **32** (6), 1719–1727.
- Fink, G., Schmid, M., Wahl, B., Wolf, T. & Wüest, A. 2014 Heat flux modifications related to climate-induced warming of large European lakes. *Water Resources Research* **50** (3), 2072–2085.
- Gächter, R. & Müller, B. 2003 Why the phosphorus retention of lakes does not necessarily depend on the oxygen supply to their sediment surface. *Limnology and Oceanography* **48** (2), 929–933.
- Gudasz, C., Bastviken, D., Steger, K., Premke, K., Sobek, S. & Tranvik, L. J. 2010 Temperature-controlled organic carbon mineralization in lake sediments. *Nature* **466** (7305), 478–481.
- Hipsey, M. R., Bruce, L. C., Boon, C., Busch, B., Carey, C. C., Hamilton, D. P., Hanson, P. C., Read, J. S., De Sousa, E. & Weber, M. 2019 A General Lake Model (GLM 3.0) for linking with high-frequency sensor data from the Global Lake Ecological Observatory Network (GLEON). *Geoscientific Model Development* **12**, 473–523.
- Holdren, G. C. & Armstrong, D. E. 1980 Factors affecting phosphorus release from intact lake sediment cores. *Environmental Science & Technology* **14** (1), 79–87.
- IPCC 2014 *Climate Change 2013: the Physical Science Basis: Working Group I Contribution to the Fifth Assessment Report of the Intergovernmental Panel on Climate Change*. Cambridge University Press.
- Ishii, Y., Harigae, S., Tanimoto, S., Yabe, T., Yoshida, T., Taki, K., Komatsu, N., Watanabe, K., Negishi, M. & Tatsumoto, H. 2010 Spatial variation of phosphorus fractions in bottom sediments and the potential contributions to eutrophication in shallow lakes. *Limnology* **11** (1), 5–16.
- Jensen, H. S. & Andersen, F. O. 1992 Importance of temperature, nitrate, and pH for phosphate release from aerobic sediments of four shallow, eutrophic lakes. *Limnology and Oceanography* **37** (3), 577–589.
- Klump, J. V. & Martens, C. S. 1981 Biogeochemical cycling in an organic rich coastal marine basin – II. Nutrient sediment-water exchange processes. *Geochimica et Cosmochimica Acta* **45** (1), 101–121.
- Li, Y.-H. & Gregory, S. 1974 Diffusion of ions in sea water and in deep-sea sediments. *Geochimica et Cosmochimica Acta* **38** (5), 703–714.
- Li, J., Jiang, Y., Xia, X. & Hu, Y. 2018 Increase of surface solar irradiance across East China related to changes in aerosol properties during the past decade. *Environmental Research Letters* **13** (3), 034006.
- Li, X., Peng, S., Deng, X., Su, M. & Zeng, H. 2019 Attribution of lake warming in four shallow lakes in the Middle and Lower Yangtze River basin. *Environmental Science & Technology* **53** (21), 12548–12555.
- Livingstone, D. M. 2003 Impact of secular climate change on the thermal structure of a large temperate central European lake. *Climatic Change* **57** (1), 205–225.
- Maberly, S. C., O'Donnell, R. A., Woolway, R. I., Cutler, M. E., Gong, M., Jones, I. D., Merchant, C. J., Miller, C. A., Politi, E. & Scott, E. M. 2020 Global lake thermal regions shift under climate change. *Nature Communications* **11** (1), 1–9.
- Masunaga, E. & Komuro, S. 2019 Stratification and mixing processes associated with hypoxia in a shallow lake (Lake Kasumigaura, Japan). *Limnology* **21**, 173–186.
- Matsuoka, Y., Goda, T. & Naito, M. 1986 An eutrophication model of Lake Kasumigaura. *Ecological Modelling* **31** (1–4), 201–219.
- Matsuzaki, S. S., Suzuki, K., Kadoya, T., Nakagawa, M. & Takamura, N. 2018 Bottom-up linkages between primary production, zooplankton, and fish in a shallow, hypereutrophic lake. *Ecology* **99** (9), 2025–2036.
- Matsuzaki, S. S.-i., Tanaka, A., Kohzu, A., Suzuki, K., Komatsu, K., Shinohara, R., Nakagawa, M., Nohara, S., Ueno, R. & Satake, K. 2021 Seasonal dynamics of the activities of dissolved <sup>137</sup>Cs and the <sup>137</sup>Cs of fish in a shallow, hypereutrophic lake: links to bottom-water oxygen concentrations. *Science of the Total Environment* **761**, 143257.
- Murphy, J. & Riley, J. P. 1962 A modified single solution method for the determination of phosphate in natural waters. *Analytica Chimica Acta* **27**, 31–36.
- Niedrist, G., Psenner, R. & Sommaruga, R. 2018 Climate warming increases vertical and seasonal water temperature differences and inter-annual variability in a mountain lake. *Climatic Change* **151** (3), 473–490.

- O'Reilly, C. M., Sharma, S., Gray, D. K., Hampton, S. E., Read, J. S., Rowley, R. J., Schneider, P., Lenters, J. D., McIntyre, P. B. & Kraemer, B. M. 2015 Rapid and highly variable warming of lake surface waters around the globe. *Geophysical Research Letters* **42** (24), 10,773–10,781.
- Pivato, M., Carniello, L., Gardner, J., Silvestri, S. & Marani, M. 2018 Water and sediment temperature dynamics in shallow tidal environments: the role of the heat flux at the sediment-water interface. *Advances in Water Resources* **113**, 126–140.
- Reddy, K. R. & DeLaune, R. D. 2008 *Biogeochemistry of Wetlands: Science and Applications*. CRC Press, Boca Raton, FL.
- Reitzel, K., Ahlgren, J., DeBrabandere, H., Waldebeck, M., Gogoll, A., Tranvik, L. & Rydin, E. 2007 Degradation rates of organic phosphorus in lake sediment. *Biogeochemistry* **82** (1), 15–28.
- Rydin, E., Kumblad, L., Wulff, F. & Larsson, P. 2017 Remediation of a eutrophic bay in the Baltic Sea. *Environmental Science & Technology* **51** (8), 4559–4566.
- Schindler, D. W. 2012 The dilemma of controlling cultural eutrophication of lakes. *Proceedings of the Royal Society B: Biological Sciences* **279** (1746), 4322–4333.
- Sinkko, H., Lukkari, K., Jama, A. S., Sihvonen, L. M., Sivonen, K., Leivuori, M., Rantanen, M., Paulin, L. & Lyra, C. 2011 Phosphorus chemistry and bacterial community composition interact in brackish sediments receiving agricultural discharges. *PLoS One* **6** (6), e21555.
- Sugita, M., Ikura, H., Miyano, A., Yamamoto, K. & Zhongwang, W. 2014 Evaporation from Lake Kasumigaura: annual totals and variability in time and space. *Hydrological Research Letters* **8** (3), 103–107.
- Sugita, M., Ogawa, S. & Kawade, M. 2020 Wind as a main driver of spatial variability of surface energy balance over a shallow 102-km<sup>2</sup> Scale Lake: Lake Kasumigaura, Japan. *Water Resources Research* **56** (8), e2020WR027173.
- Tanaka, K., Ohmura, A., Folini, D., Wild, M. & Ohkawara, N. 2016 Is global dimming and brightening in Japan limited to urban areas? *Atmospheric Chemistry and Physics* **16** (21), 13969.
- Tsuchiya, K., Komatsu, K., Shinohara, R., Imai, A., Matsuzaki, S. i. S., Ueno, R., Kuwahara, V. S. & Kohzu, A. 2020 Variability of benthic methane-derived carbon along seasonal, biological, and sedimentary gradients in a polymictic lake. *Limnology and Oceanography* **65** (12), 3017–3031.
- Veraart, A. J., De Klein, J. J. & Scheffer, M. 2011 Warming can boost denitrification disproportionately due to altered oxygen dynamics. *PLoS One* **6** (3), e18508.
- Wang, M., Xu, X., Wu, Z., Zhang, X., Sun, P., Wen, Y., Wang, Z., Lu, X., Zhang, W. & Wang, X. 2019 Seasonal pattern of nutrient limitation in a Eutrophic lake and quantitative analysis of the impacts from internal nutrient cycling. *Environmental Science & Technology* **53** (23), 13675–13686.
- Wild, M. 2009 Global dimming and brightening: a review. *Journal of Geophysical Research: Atmospheres* **114** (D10), D00D16.
- Wild, M., Gilgen, H., Roesch, A., Ohmura, A., Long, C. N., Dutton, E. G., Forgan, B., Kallis, A., Russak, V. & Tsvetkov, A. 2005 From dimming to brightening: decadal changes in solar radiation at Earth's surface. *Science* **308** (5723), 847–850.
- Winslow, L. A., Read, J. S., Hansen, G. J., Rose, K. C. & Robertson, D. M. 2017 Seasonality of change: summer warming rates do not fully represent effects of climate change on lake temperatures. *Limnology and Oceanography* **62** (5), 2168–2178.
- Woolway, R. I., Weyhenmeyer, G. A., Schmid, M., Dokulil, M. T., de Eyto, E., Maberly, S. C., May, L. & Merchant, C. J. 2019 Substantial increase in minimum lake surface temperatures under climate change. *Climatic Change* **155** (1), 81–94.
- Woolway, R. I., Kraemer, B. M., Lenters, J. D., Merchant, C. J., O'Reilly, C. M. & Sharma, S. 2020 Global lake responses to climate change. *Nature Reviews Earth & Environment* **1**, 388–403.
- Yang, C., Yang, P., Geng, J., Yin, H. & Chen, K. 2020 Sediment internal nutrient loading in the most polluted area of a shallow eutrophic lake (Lake Chaohu, China) and its contribution to lake eutrophication. *Environmental Pollution* **262**, 114292.

First received 11 April 2021; accepted in revised form 11 June 2021. Available online 25 June 2021